Dyes and Pigments 99 (2013) 588–593

Contents lists available at SciVerse ScienceDirect

Dyes and Pigments

journal homepage: www.elsevier.com/locate/dyepig

Binding of sulforhodamine B to human serum albumin: A spectroscopic study

Masanori Kitamura [a], Koji Murakami [a], Kohei Yamada [a], Keiichi Kawai [b], Munetaka Kunishima [a,*]

[a] Faculty of Pharmaceutical Sciences, Institute of Medical, Pharmaceutical, and Health Sciences, Kanazawa University, Kakuma-machi, Kanazawa 920-1192, Japan
[b] Faculty of Health Sciences, Institute of Medical, Pharmaceutical, and Health Sciences, Kanazawa University, 5-11-80 Kodatsuno, Kanazawa 920-0942, Japan

ARTICLE INFO

Article history:
Received 6 March 2013
Received in revised form
20 April 2013
Accepted 13 June 2013
Available online 22 June 2013

Keywords:
Sulforhodamine B
Human serum albumin
Fluorescence
Fluorescence quenching
Circular dichroism
Albumin

ABSTRACT

Sulforhodamine B (SRB) is a widely used fluorescent dye in biological sciences including *in vivo* studies. In this study, the binding interaction between SRB and human serum albumin (HSA) was investigated by fluorescence and circular dichroism spectroscopy. Complexation with HSA leads to an increase in dye fluorescence, from which the binding constant (1.6×10^5 M^{-1} at 25 °C), binding stoichiometry (1:1), and thermodynamic parameters of the SRB–HSA interaction (ΔH = 5.2 kJ/mol, ΔS = 116.5 J/mol K) were obtained. The large positive ΔS and the small positive ΔH indicate an entropy-driven binding process, suggesting that SRB binds to Sudlow site I of HSA by a dominant hydrophobic interaction. Circular dichroism revealed some degree of conformational changes in HSA upon binding.

1. Introduction

Sulforhodamine B (SRB) shown in Chart 1 has advantageous spectral characteristics, such as high molar extinction coefficient [1], high fluorescence quantum yield [1,2], pH-independent emission [3,4], and narrow-band laser performance [5]. In addition, SRB also has considerable photostability [5,6], high water solubility [7], and low biological toxicity [8]. Therefore, it has been extensively used as a dye during the past few decades in laser technology [5,6], the food coloring industry [9,10], and especially in biological sciences [7,11–23]. The SRB assay is a well-known method to measure drug-induced cytotoxicity and cell proliferation *in vitro* for large-scale screening applications [11–13]. SRB has also been applied to study cell–cell communications [14] and neuronal morphology [15,16] and to model hydrophilic drugs *in vitro* [7,17–19]. Recently, the *in vivo* imaging of elastic and collagen fibers was developed using SRB and two-photon excitation microscopy [20]. This technique allows the noninvasive visualization of living tissue at high depths, because near infrared light is only weakly absorbed by tissue and water (e.g., the optical window in biological tissue). Interestingly, SRB can cross the blood–brain barrier after intravenous injection, and the two-photon excitation method using SRB was also exploited for the imaging of astrocyte cells in the brains of mice [21–23]. Because of the rapid increase in SRB usage, it is possible that SRB will be used for the fluorescence imaging of the human body. Hence, it is essential to understand the interaction of SRB with human serum albumin (HSA) in the blood.

HSA is the most abundant protein in plasma, which consists of approximately half of the proteins found in human blood, with a concentration of approximately 6.0×10^{-4} M [24]. One of its functions is to carry various exo- and endogenous compounds, such as fatty acids, bilirubin, tryptophan, steroids, and drugs, via two major binding sites in subdomains IIA and IIIA, namely Sudlow sites I and II, respectively. The fact that HSA can bind to dyes is evidenced by the numerous studies of the binding of various organic dyes with HSA [25–29]. However, one study concluded that SRB does not bind to the plasma albumin of mice, but experimental details were not provided [20]. In this context, it is worth studying the binding between SRB and HSA.

In this study, we report the experimental study of the binding of SRB with HSA at physiological pH using steady-state fluorescence and circular dichroism spectroscopy. The binding parameters, the

* Corresponding author. Tel./fax: +81 76 264 6201.
E-mail address: kunisima@p.kanazawa-u.ac.jp (M. Kunishima).

0143-7208/$ – see front matter © 2013 Elsevier Ltd. All rights reserved.
http://dx.doi.org/10.1016/j.dyepig.2013.06.011

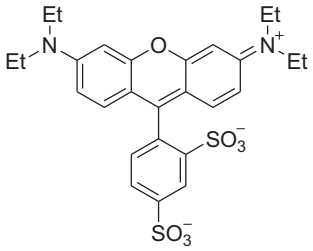

Chart 1. Structure of SRB.

identification of binding sites, and the nature of forces in the interaction will be beneficial for the use of SRB in the food coloring industry and in diagnostic imaging.

2. Experimental

2.1. Materials

Human serum albumin (free of fatty acids) was purchased from Seracare Life Sciences, and sulforhodamine B (C.I. Acid Red 52, laser grade, 95%) was obtained from Aldrich, and both were used without further purification. Deionized water was generated by an Elix UV System from Millipore.

2.2. Instrumentation

Absorption and circular dichroism spectra were recorded on a Shimadzu UV-2400PC spectrophotometer and JASCO J-820 spectrometer, respectively. Fluorescence spectra were measured on a JASCO FP-6500 spectrofluorometer equipped with an ETC-273T thermostatic cell holder using a 1.0 cm path length quartz cell.

2.3. Procedures

2.3.1. Inner-filter effect of SRB during the measurement of fluorescence from HSA

When the fluorescence spectra of HSA were measured (excitation wavelength = 295 nm, emission wavelength = 340 nm) for the Stern–Volmer plot, the intensities were corrected for the absorption of the exciting light and the reabsorption of the emitted light to decrease the inner-filter effect by using equation (1) [30–32].

$$F_{\text{corrected}} = F_{\text{observed}} \times \text{antilog}[(A_{\text{ex}} + A_{\text{em}})/2], \quad (1)$$

where $F_{\text{corrected}}$ is the corrected fluorescence value, F_{observed} is the measured fluorescence value, A_{ex} and A_{em} are the absorbance of the system at the excitation wavelength (295 nm) and at the emission wavelength (340 nm), respectively.

2.3.2. Binding studies between HSA and SRB

Stock solutions of SRB and HSA were prepared with suitable concentrations for each experiment. The interactions between SRB and HSA were monitored by fluorescence and circular dichroism spectroscopic techniques.

3. Results and discussion

3.1. Fluorescence characteristics of SRB upon complexation with HSA

Fluorescence measurements can provide some information on the binding of small molecules to proteins, such as binding constants, binding sites, binding modes, binding mechanisms, and inter molecular distances. The fluorescence intensity of SRB is sensitive to environmental solvent polarity [2,33]. For example, the fluorescence quantum yield of SRB in water ($\Phi = 0.39$) is smaller than that in a mixture of water and dioxane ($\Phi = 0.79$ where water/dioxane = 2:98) [2]. 1-Anilinonaphthalene-6-sulfonic acid (ANS) is weakly or non-fluorescent in water but strongly fluoresces when bound to HSA or bovine serum albumin (BSA) [34]. As was observed in ANS, the fluorescence intensity of SRB also increased upon the addition of HSA (Fig. 1), indicating microenvironmental changes around SRB and the inclusion complexation of SRB by HSA. As shown in Fig. 2, the continuous variation method (Job's plot) using fluorescence from SRB suggests 1:1 inclusion complexation stoichiometry between SRB and HSA [35,36]. This fluorescence spectral change of SRB in the presence of HSA was also analyzed by the Scatchard equation (2):

$$r/D_f = nK - rK, \quad (2)$$

where r represents the number of moles of bound SRB per mole of HSA, D_f shows the molar concentration of free SRB, n and K are the number of binding sites and the binding constant, respectively. From the Scatchard plot of the SRB–HSA system at 25 °C (Fig. 3), the binding constant between SRB and HSA was estimated as $1.6 \times 10^5\ M^{-1}$. Table 1 summarizes the binding constants at various temperatures (15–35 °C).

3.2. Binding mode

If the enthalpy change (ΔH) does not vary significantly in the temperature range, both enthalpy change and entropy change (ΔS) can be calculated from the van 't Hoff equation (3):

$$\ln K = -\Delta H/RT + \Delta S/R, \quad (3)$$

where K is the binding constant at the corresponding temperature, and R is the gas constant. The ΔG, ΔH, and ΔS values for SRB–HSA complexation are obtained from Fig. 4 and are listed in Table 1.

There are several types of non-covalent interaction modes between a small molecule and a protein, including hydrogen bonding, electrostatic interaction, van der Waals force, and hydrophobic interaction. The binding modes of Sudlow site I with small molecules are mainly by hydrophobic interactions, whereas those of Sudlow site II involve a combination of hydrophobic, hydrogen bonding, and electrostatic interactions [37,38]. A positive ΔS and insignificant ΔH value frequently suggest hydrophobic interaction,

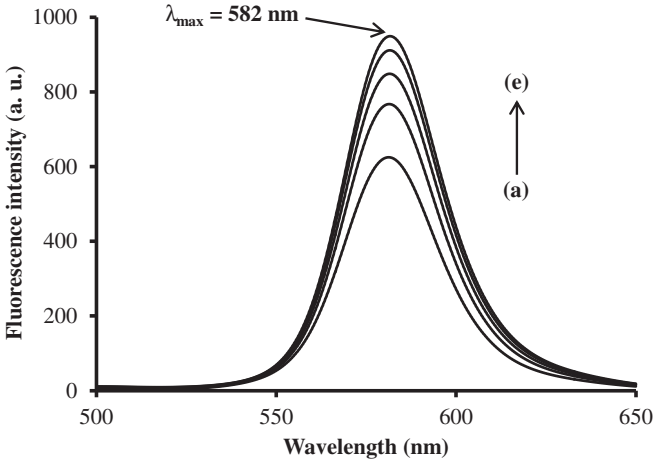

Fig. 1. Fluorescence spectral change of SRB (5 μM) in the presence of HSA (0–16 μM) in phosphate buffer (67 mM, pH 7.4) at 25 °C (excitation at 425 nm). The HSA concentrations were (a) 0, (b) 4, (c) 8, (d) 12, and (e) 16 μM.

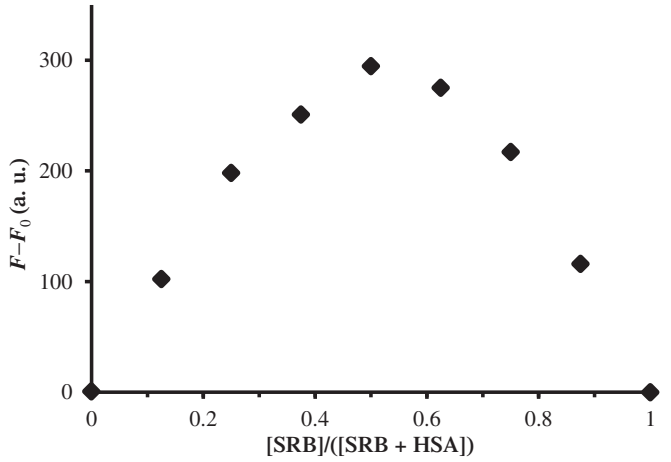

Fig. 2. Job's plot of SRB bound to HSA in phosphate buffer (67 mM, pH 7.4) at 25 °C (excitation at 425 nm, emission at 625 nm). [SRB + HSA] = 40 μM. F_0 and F are the fluorescence intensities of SRB in the absence and presence of HSA, respectively.

where water molecules arranged in an orderly manner around a small molecule and a protein are released and are disordered [39]. The large positive ΔS and the small positive ΔH shown in Table 1 indicate an entropy-driven binding process of amphiphilic SRB [40], implying that the binding of SRB to Sudlow site I of HSA is similar to that of warfarin [41,42] and azidothymidine (AZT) [43] to the site I and exhibits similar thermodynamic parameters.

3.3. Fluorescence quenching of HSA

Fluorescence quenching refers to the decrease in the fluorescence quantum yield of a fluorophore due to various molecular interactions, including excited-state interactions, molecular rearrangements, energy transfer, ground–state complex formation, and collisional quenching. The intrinsic fluorescence of HSA is mainly attributable to the single tryptophan residue (Trp-214) located at the center of its hydrophobic interior adjacent to a hinge region (Sudlow site I) [44]. Compounds that bind to Sudlow site I often diminish the HSA fluorescence and it was used to investigate the interaction of drugs with HSA [44–46]. The decrease in the fluorescence intensity is analyzed by the Stern–Volmer equation (4):

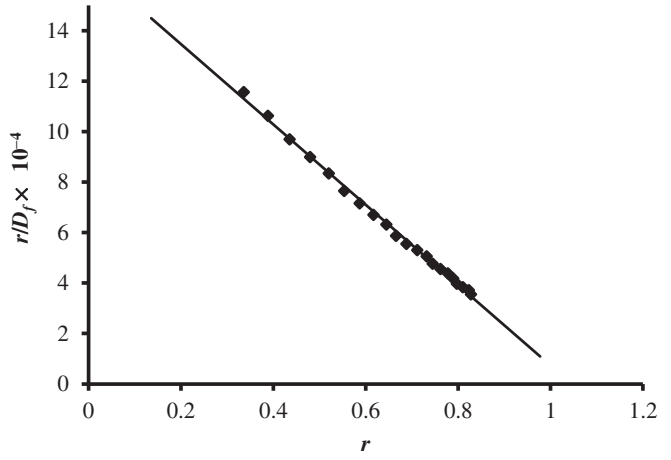

Fig. 3. Scatchard plot of SRB binding to HSA at 25 °C and pH 7.4 (phosphate buffer, 67 mM). r indicates the number of moles of SRB bound per mole of HSA. D_f indicates the free SRB concentration. The SRB concentrations were varied from 10 to 40 μM at different HSA concentrations (0, 34, or 150 μM). Fluorescence measurements of SRB were carried out under the following conditions: excitation at 425 nm and emission at 625 nm.

Table 1
Binding constants obtained from Scatchard plots and thermodynamic parameters of the SRB–HSA interaction at pH 7.4.

T (K)	log K	n	ΔG (kJ/mol)	ΔH (kJ/mol)	ΔS (J/mol K)
288	5.1	1.03	−28.3	5.2	116.5
298	5.2	1.05	−29.7		
308	5.2	1.00	−30.7		

$$F_0/F = 1 + K_{sv}[Q], \tag{4}$$

where F_0 and F indicate the steady-state fluorescence intensities in the absence and in the presence of a quencher (i.e., SRB), respectively, K_{sv} is the Stern–Volmer quenching constant, and [Q] is the quencher concentration. The Stern–Volmer plot (Fig. 5) shows $K_{sv} = 1.1 \times 10^4\ M^{-1}$, and the apparent quenching rate constant k_q^{app} is calculated according to $k_q^{app} = K_{sv}/\tau_0$, where τ_0 is the lifetime of the fluorophore (i.e., HSA) in the absence of quencher (τ_0 of HSA is approximately 10^{-8} s) [46]. The k_q^{app} value of $1.1 \times 10^{12}\ M^{-1}\ s^{-1}$ is higher than the maximum diffusion-limited rate, implying that static quenching caused by complex formation plays a dominant role in this quenching process, rather than collisional quenching.

3.4. Circular dichroism

Circular dichroism (CD) spectral measurement is often utilized to monitor the conformational changes in HSA upon the complexation of small molecules [47,48]. The CD spectra of HSA exhibit a typical shape of an α-helix-rich secondary structure with two minima at approximately 208 and 222 nm. The CD spectra results upon the addition of SRB are expressed as the mean residue ellipticity (MRE) defined by equation (5):

$$\text{MRE} = \textit{observed CD}/(c \times n \times l), \tag{5}$$

where c is the molar concentration of HSA, n is the number of amino acid residues (585), and l is the path length (1 cm). The spectral change in Fig. 6 is indicative of SRB–HSA complexation and the loss of α-helix.

3.5. Energy transfer

The fluorescence and CD spectra studies proved that HSA forms a complex with SRB. Resonance energy transfer (RET) has been utilized for measuring molecular distances in biological and

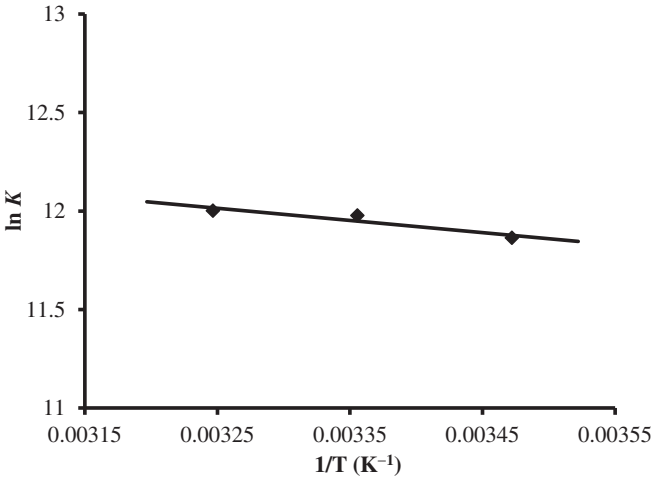

Fig. 4. van't Hoff plots of the HSA–SRB interaction.

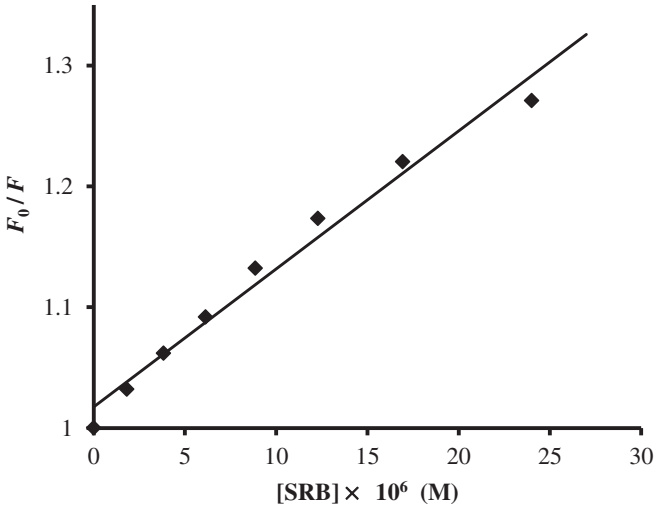

Fig. 5. Stern–Volmer plot of the fluorescence quenching of HSA (10 μM) upon the addition of SRB at 25 °C and pH 7.4 (phosphate buffer, 67 mM). Excitation and emission wavelengths were 295 and 340 nm, respectively. F_0 and F are the corrected fluorescence intensities of HSA in the absence and presence of SRB due to the inner-filter effect, respectively (See Experimental Section).

macromolecular systems [49–52]. RET occurs when the fluorescence emission spectra of a donor (HSA) overlap with the absorption spectra of an acceptor (SRB), as depicted in Fig. 7. By using equation (6) for RET, the distance r between Trp-214 of HSA and SRB is calculated.

$$E = 1 - F/F_0 = R_0^6/\left(R_0^6 + r^6\right), \tag{6}$$

E denotes the efficiency of transfer between the donor and the acceptor, r is the average distance between the donor and acceptor, and R_0, known as the Förster distance, is the critical distance when the efficiency of transfer is 50%. R_0 can be obtained from equation (7):

$$R_0^6 = 8.79 \times 10^{-25} \times K^2 \times n^{-4} \times \varphi \times J, \tag{7}$$

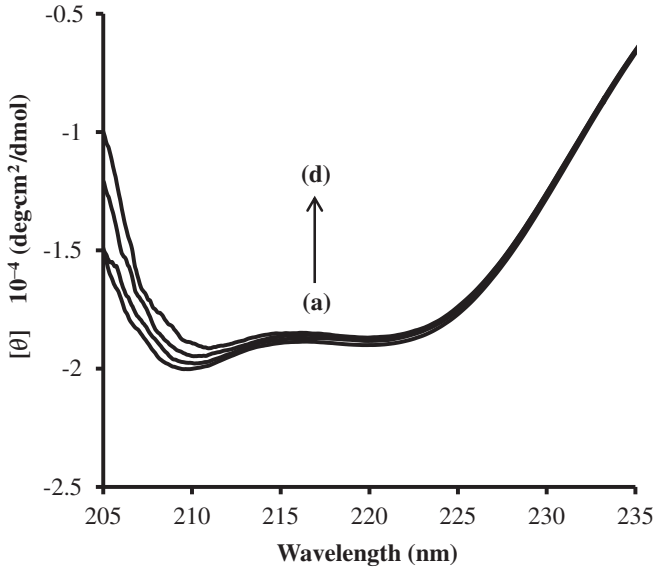

Fig. 6. CD spectra of HSA (1 μM) at 25 °C and pH 7.4 (phosphate buffer, 67 mM). The SRB concentrations were (a) 0, (b) 7.8, (c) 15.1, and (d) 22.1. Results are expressed as mean residue ellipticity (MRE) in deg·cm²/dmol.

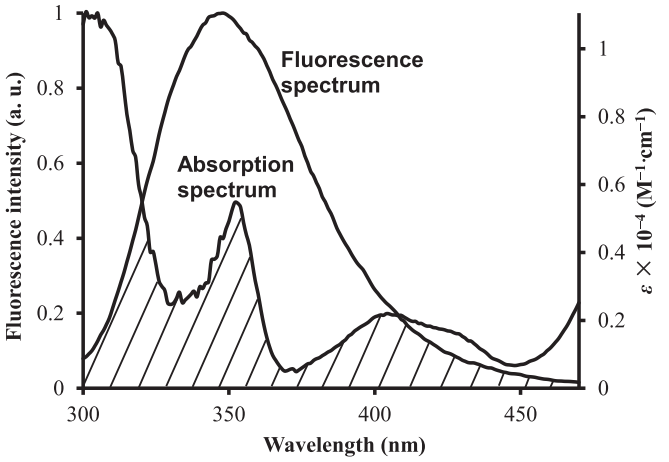

Fig. 7. Spectral overlap between the absorption spectrum of SRB and the fluorescence spectrum of HSA (25 °C and pH 7.4).

K^2 is the orientation factor related to the geometry of the donor and acceptor dipoles, and $K^2 = 2/3$ for random orientation, n is the average refractive index of the medium in the wavelength range in which spectral overlap is significant, φ is the fluorescence quantum yield of the donor (0.118 for HSA), and J is the spectral overlap between the emission spectrum of the donor and the absorption spectrum of the acceptor, which are calculated using equation (8):

$$J = \int_0^\infty F(\lambda)\varepsilon(\lambda)\lambda^4 \mathrm{d}\lambda / \int_0^\infty F(\lambda)\mathrm{d}\lambda, \tag{8}$$

where $F(\lambda)$ is the corrected fluorescence intensity of the donor in the wavelength range, $\varepsilon(\lambda)$ is the molar absorptivity of the acceptor at the wavelength λ. Applying equations (6)–(8), we calculate $R_0 = 2.15$ nm, $E = 0.28$, and $r = 2.51$ nm. The R_0 and r values are on the 2–8 nm scale, and $0.5R_0 < r < 1.5R_0$, indicating the existence of an interaction between SRB and Trp-214 of HSA.

3.6. Binding site

To study the distinct binding site for SRB on HSA, site-specific ligands were used: warfarin and furosemide for site I and

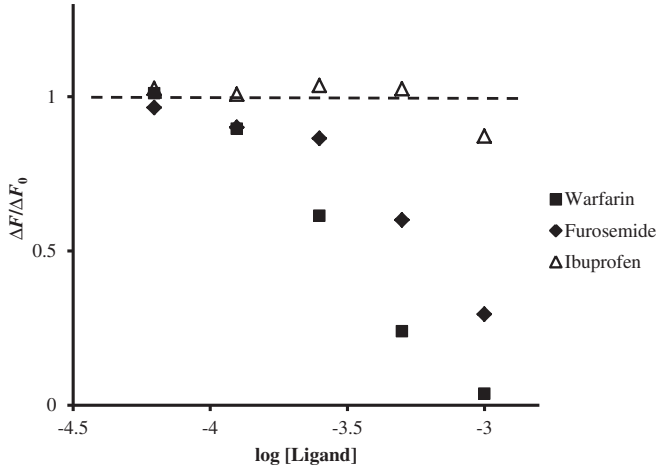

Fig. 8. Change in fluorescence spectra of SRB (5 μM) bound to HSA (90 μM) upon the addition of ligand molecules (warfarin, ibuprofen, or furosemide) at 25 °C and pH 7.4 (phosphate buffer, 67 mM). Excitation and emission wavelengths were 425 and 581 nm, respectively. F_0 and F are the fluorescence intensities of HSA in the absence and presence of SRB, respectively.

ibuprofen for site II [53–56]. Fig. 8 shows that the fluorescence intensity significantly decreased after the addition of warfarin and furosemide but not after adding ibuprofen, suggesting that SRB binds to site I of HSA. It could be presumed that xanthene moiety of the SRB is situated in the hydrophobic cavity of the site I and two sulfonates slightly interact with positively charged residues such as Lys-195, Lys-199, Arg-218, Arg-222, His-242, and Arg-257 which are located at the entrance of the site I cavity.

4. Conclusions

This study presents fluorescence and circular dichroism spectroscopic results of the interaction of SRB with HSA. The increase in the fluorescence intensity of SRB upon complexation with HSA revealed the binding constant (1.6×10^5 M^{-1} at 25 °C), binding stoichiometry (1:1), and thermodynamic parameters of the SRB–HSA interaction ($\Delta H = 5.2$ kJ/mol, $\Delta S = 116.5$ J/mol K). The entropy-driven binding process (large positive ΔS and small positive ΔH) implies that SRB binds to Sudlow site I of HSA predominantly by hydrophobic interaction. This site-selective binding was confirmed by site-competitive binding experiments using warfarin and furosemide as marker ligands for site I and ibuprofen for site II. Circular dichroism suggested some degree of conformational changes in HSA upon binding with SRB. Since HSA is an important biomarker for clinical practice, SRB could be an alternative to bromocresol green or bromocresol purple for the measurement of HSA. The results and data presented here provide important insights into the interaction of SRB with HSA under physiological conditions, and the use of SRB should be beneficial in the food coloring industry and in diagnostic imaging.

Appendix A. Supplementary data

Supplementary data related to this article can be found at http://dx.doi.org/10.1016/j.dyepig.2013.06.011.

References

[1] Drake JM, Morse RI, Steppel RN, Young D. Kiton red S and rhodamine B. The spectroscopy and laser performance of red laser dyes. Chem Phys Lett 1975;35:181–8.
[2] Ishizaka S, Kim H-B, Kitamura N. Time-resolved total internal reflection fluorometry study on polarity at a liquid/liquid interface. Anal Chem 2001;73:2421–8.
[3] Berkland C, Pollauf E, Raman C, Silverman R, Kim K, Pack DW. Macromolecule release from monodisperse PLG microspheres: control of release rates and investigation of release mechanism. J Pharm Sci 2007;96:1176–91.
[4] Coppeta J, Rogers C. Dual emission laser induced fluorescence for direct planar scalar behavior measurements. Exp Fluids 1998;25:1–15.
[5] Jagtap KK, Ray AK, Pardeshi SK, Dasgupta K. Kiton red S dye: Photophysical, photostability, photothermal and narrow-band laser performances using different solvents. Pramana – J Phys 2010;75:991–8.
[6] Hay J, Ranson C, Sugden JK. Photochemical stability of sulphorhodamine B. Dyes Pigm 1995;27:55–61.
[7] Yu B, Dong C-Y, So PTC, Blankschtein D, Langer R. *In vitro* visualization and quantification of oleic acid induced changes in transdermal transport using two-photon fluorescence microscopy. J Invest Dermatol 2001;117:16–25.
[8] Chodosh J, Dix RD, Howell RC, Stroop WG, Tseng SCG. Staining characteristics and antiviral activity of sulforhodamine B and lissamine green B. Invest Ophthalmol Vis Sci 1994;35:1046–58.
[9] Oka H, Ikai Y, Kawamura N, Hayakawa J, Yamada M, Harada K, et al. Purification of food color red no. 106 (acid red) using high-speed counter-current chromatography. J Chromatogr A 1991;538:149–56.
[10] Oka H, Suzuki M, Harada K, Iwaya M, Fujii K, Goto T, et al. Purification of food color red no. 106 (acid red) using pH-zone-refining counter-current chromatography. J Chromatogr A 2002;946:157–62.
[11] Skehan P, Storeng R, Scudiero D, Monks A, Mcmahon J, Vistica D, et al. New colorimetric cytotoxicity assay for anticancer-drug screening. J Natl Cancer Inst 1990;82:1107–12.
[12] Voigt W. Sulforhodamine B assay and chemosensitivity. In: Blumenthal RD, editor. Methods in molecular medicine. Chemosensitivity vol. 1, In Vitro assays, vol. 110. Totowa: Humana Press; 2005. p. 39–48.
[13] Pauwels B, Korst AEC, de Pooter CMJ, Pattyn GGO, Lambrechts HAJ, Baay MFD, et al. Comparison of the sulforhodamine B assay and the clonogenic assay for in vitro chemoradiation studies. Cancer Chemother Pharmacol 2003;51:221–6.
[14] Safranyos RGA, Caveney S, Miller JG, Petersen NO. Relative roles of gap junction channels and cytoplasma in cell-to-cell diffusion of fluorescent tracers. Proc Natl Acad Sci USA 1987;84:2272–6.
[15] Bank M, Schacher S. Segregation of presynaptic inputs on an identified target neuron in vitro: structural remodeling visualized over time. J Neurosci 1992;12:2960–72.
[16] Zhu H, Wu F, Schacher S. *Aplysia* cell adhesion molecules and serotonin regulate sensory cell-motor cell interactions during early stages of synapse formation in vitro. J Neurosci 1994;14:6886–900.
[17] Shen Z, Mitragotri S. Intestinal patches for oral drug delivery. Pharm Res 2002;19:391–5.
[18] Jiang J, Geroski DH, Edelbauser HF, Prausnitz MR. Measurement and prediction of lateral diffusion within human sclera. Invest Ophthalmol Vis Sci 2006;47:3011–6.
[19] Bender J, Simonsson C, Smedh M, Engström S, Ericson MB. Lipid cubic phases in topical drug delivery: Visualization of skin distribution using two-photon microscopy. J Control Release 2008;129:163–9.
[20] Richard C, Vial J-C, Douady J, van der Sanden B. In vivo imaging of elastic fibers using sulforhodamine B. J Biomed Opt 2007;12:064017.
[21] Vérant P, Ricard C, Serduc R, Vial J-C, van der Sanden B. *In vivo* staining of neocortical astrocytes via the cerebral microcirculation using sulforhodamine B. J Biomed Opt 2008;13:064028.
[22] Vérant P, Serduc R, van der Sanden B, Chantal R, Ricard C, Coles JA, et al. Subtraction method for intravital two-photon microscopy: intraparenchymal imaging and quantification of extravasation in mouse brain cortex. J Biomed Opt 2008;13:011002.
[23] Appaix F, Girod S, Boisseau S, Römer J, Vial J-C, Albrieux M, et al. Specific in vivo staining of astrocytes in the whole brain after intravenous injection of sulforhodamine dyes. PLoS One 2012;7:e35169.
[24] Kratz F, Elsadek B. Clinical impact of serum proteins on drug delivery. J Control Release 2012;161:429–45.
[25] Yang Q, Zhou X, Chen X. Combined molecular docking and multi-spectroscopic investigation on the interaction between Eosin B and human serum albumin. J Lumin 2011;131:581–6.
[26] Zhang G, Ma Y. Mechanistic and conformational studies on the interaction of food dye amaranth with human serum albumin by multispectroscopic methods. Food Chem 2013;136:442–9.
[27] Yue Y, Chen X, Qin J, Yao X. A study of the binding of C.I. Direct yellow 9 to human serum albumin using optical spectroscopy and molecular modeling. Dyes Pigm 2008;79:176–82.
[28] Song S, Hou X, Wu Y, Shuang S, Yang C, Inoue Y, et al. Study on the interaction between methyl blue and human serum albumin by fluorescence spectrometry. J Lumin 2009;129:169–75.
[29] Ding F, Li N, Han B, Liu F, Zhang L, Sun Y. The binding of C.I. Acid Red 2 to human serum albumin: determination of binding mechanism and binding site using fluorescence spectroscopy. Dyes Pigm 2009;83:249–57.
[30] Lakowicz JR. Principles of fluorescence spectroscopy. 3rd ed. New York: Springer Science+Business Media; 2006. p. 55–6.
[31] Kubista M, Sjöback R, Eriksson S, Albinsson B. Experimental correction for the inner-filter effect in fluorescence spectra. Analyst 1994;119:417–9.
[32] Yappert MC, Ingle JD. Correction of polychromatic luminescence signals for inner-filter effects. Appl Spectrosc 1989;43:759–67.
[33] Martín V, Costela A, Pintado-Sierra M, García-Moreno I. Sulforhodamine B doped polymeric matrices: a high efficient and stable solid-state laser. J Photochem Photobiol A 2011;219:265–72.
[34] Lakowicz JR. Principles of fluorescence spectroscopy. 3rd ed. New York: Springer Science+Business Media; 2006. p. 71–2.
[35] Connors KA. Binding constants. New York: John Wiely & Sons, Inc; 1987. p. 24–8.
[36] Zhou Y, Yu H, Zhang L, Sun J, Wu L, Lu Q, et al. Host properties of cucurbit [7] uril: fluorescence enhancement of acridine orange. J Incl Phenom Macrocycl Chem 2008;61:259–64.
[37] Zhong D, Douhal A, Zewail AH. Femtosecond studies of protein–ligand hydrophobic binding and dynamics: human serum albumin. Proc Natl Acad Sci USA 2000;97:14056–61.
[38] Urien S, Nguyen P, Berlioz S, Brée F, Vacherot F, Tillement J-P. Characterization of discrete classes of binding sites of human serum albumin by application of thermodynamic principles. Biochem J 1994;302:69–72.
[39] Guo Y, Yue Q, Gao B. Probing the molecular mechanism of C.I. Acid red 73 binding to human serum albumin. Environ Toxicol Pharmacol 2010;30:45–51.
[40] Polat BE, Lin S, Mendenhall JD, VanVeller B, Langer R, Blankschtein D. Experimental and molecular dynamics investigation into the amphiphilic nature of sulforhodamine B. J Phys Chem B 2011;115:1394–402.
[41] Maes V, Engelborghs Y, Hoebeke J, Maras Y, Vercruysse A. Fluorimetric analysis of the binding of warfarin to human serum albumin. Equilibrium and kinetic study. Mol Pharmacol 1982;21:100–7.
[42] Oester YT, Keresztes-Nagy S, Mais RF, Becktel J, Zaroslinski JF. Effect of temperature on binding of warfarin by human serum albumin. J Pharm Sci 1976;65:1673–7.
[43] Quevedo MA, Moroni GN, Briñón MC. Human serum albumin binding of novel antiretroviral nucleoside derivatives of AZT. Biochem Biophys Res Commun 2001;288:954–60.

[44] Matei I, Hillebrand M. Interaction of kaempferol with human serum albumin: a fluorescence and circular dichroism study. J Pharm Biomed Anal 2010;51:768–73.
[45] Trynda-Lemiesz L, Wiglusz K. Interactions of human serum albumin with meloxicam: characterization of binding site. J Pharm Biomed Anal 2010;52:300–4.
[46] Yang F, Yue J, Ma L, Ma Z, Li M, Wu X, et al. Interactive associations of drug–drug and drug–drug–drug with IIA subdomain of human serum albumin. Mol Pharmaceutics 2012;9:3259–65.
[47] Stan D, Matei I, Mihailescu C, Savin M, Matache M, Hillebrand M, et al. Spectroscopic investigations of the binding interaction of a new indanedione derivative with human and bovine serum albumins. Molecules 2009;14:1614–26.
[48] Varlan A, Hillebrand M. Bovine and human serum albumin interactions with 3-carboxyphenoxathiin studied by fluorescence and circular dichroism spectroscopy. Molecules 2010;15:3905–19.
[49] Kandagal PB, Ashoka S, Seetharamappa J, Shaikh SMT, Jadegoud Y, Ijare OB. Study of the interaction of an anticancer drug with human and bovine serum albumin: spectroscopic approach. J Pharm Biomed Anal 2006;41:393–9.
[50] Matei I, Ionescu S, Hillebrand M. Interaction of fisetin with human serum albumin by fluorescence, circular dichroism spectroscopy and DFT calculations: binding parameters and conformational changes. J Lumin 2011;131:1629–35.
[51] Das P, Mallick A, Haldar B, Chakrabarty A, Chattopadhyay N. Fluorescence resonance energy transfer from tryptophan in human serum albumin to a bioactive indoloquinolizine system. J Chem Sci 2007;119:77–82.
[52] Chatterjee T, Pal A, Dey S, Chatterjee BK, Chakrabarti P. Interaction of virstatin with human serum albumin: spectroscopic analysis and molecular modeling. PLoS ONE 2012;7:e37468.
[53] Hu Y-J, Ou-Yang Y, Dai C-M, Liu Y, Xiao X-H. Site-selective binding of human serum albumin by palmatine: spectroscopic approach. Biomacromolecules 2010;11:106–12.
[54] Joseph KS, Moser AC, Basiaga SBG, Schiel JE, Hage DS. Evaluation of alternatives to warfarin as probes for Sudlow site I of human serum albumin: characterization by high-performance affinity chromatography. J Chromatogr A 2009;1216:3492–500.
[55] Basken NE, Mathias CJ, Green MA. Elucidation of the human serum albumin (HSA) binding site for the Cu-PTSM and Cu-ATSM radiopharmaceuticals. J Pharma Sci 2009;98:2170–9.
[56] Li S, Yao D, Bian H, Chen Z, Yu J, Yu Q, et al. Interaction between plumbagin and human serum albumin by fluorescence spectroscopy. J Solution Chem 2011;40:709–18.